# Chapter 1

# Nonequilibrium dynamical mean-field theory of strongly correlated electrons

V. Turkowski

*Department of Physics and Astronomy, University of Missouri-Columbia, Columbia, MO 65202, USA*
*turkowskiv@missouri.edu*

J.K. Freericks

*Department of Physics, Georgetown University, Washington, D.C. 20057, USA*
*freericks@physics.georgetown.edu*

We present a review of our recent work in extending the successful dynamical mean-field theory from the equilibrium case to nonequilibrium cases. In particular, we focus on the problem of turning on a spatially uniform, but possibly time varying, electric field (neglecting all magnetic field effects). We show how to work with a manifestly gauge-invariant formalism, and compare numerical calculations from a transient-response formalism to different types of approximate treatments, including the semiclassical Boltzmann equation and perturbation theory in the interaction. In this review, we solve the nonequilibrium problem for the Falicov-Kimball model, which is the simplest many-body model and the easiest problem to illustrate the nonequilibrium behavior in both diffusive metals and Mott insulators. Due to space restrictions, we assume the reader already has some familiarity both with the Kadanoff-Baym-Keldysh nonequilibrium formalism and with equilibrium dynamical mean-field theory; we provide a guide to the literature where additional details can be found.

## 1.1. Introduction

Dynamical mean-field theory (DMFT) was introduced in 1989[1] shortly after Metzner and Vollhardt[2] proposed scaling the hopping matrix element as the inverse square root of the spatial dimension to achieve a nontriv-

ial limit where the many-body dynamics are local. Since then, the field has blossomed to the point where nearly all model many-body problems have now been solved,[3] and much recent work has focused on applying DMFT principles to real materials calculations.[4] Little work has emphasized nonequilibrium aspects of the many-body problem, where the strongly correlated system is driven by an external field that can possibly sustain a nonequilibrium steady state. In this contribution, we will review recent work that has been completed on expanding DMFT approaches into the nonequilibrium realm. We will show how to work with so-called gauge-invariant Green functions[5] to illustrate that one can carry out calculations in a form that manifestly is independent of the gauge chosen to describe the driving fields. This approach is different from our previously published work, where we worked solely with Green functions in the Hamiltonian gauge (where the scalar potential vanishes).

We examine the problem of strongly correlated electrons driven by a spatially uniform electric field in the limit of infinite dimensions,[6–8] where DMFT can be applied to solve the problem exactly. In infinite dimensions, the self-energy of the electrons is local, and the lattice problem can be mapped onto the problem of an impurity coupled to an effective time-dependent field (which is adjusted so that the impurity Green function and the local Green function on the lattice are identical). The impurity problem in the dynamical mean field can be solved exactly for many different cases. In equilibrium, a large number of strongly correlated models have been solved in infinite dimensions, like the Falicov-Kimball model,[1,10,11] the Hubbard model,[12–14] the periodic Anderson model,[15,16] and the Holstein model,[17,18] (for a reviews, see Refs. 3 and 19). Recently, there has been a significant effort in combining DMFT with density functional theory (DFT) to describe properties of real materials when DFT is insufficient to properly describe the electron-electron interactions (see Ref. 4 for a review). It is now generally believed that DMFT is a good approximation to the many-body problem in three dimensions, and it can accurately describe strong electron-electron correlation effects in bulk systems.

The first attempt to employ DMFT to describe nonequilibrium properties of a strongly correlated model was made by Schmidt and Monien in Ref. 20, where they studied the spectral properties of the Hubbard model in the presence of a time-dependent chemical potential by using iterated perturbation theory (PT). Recently, we have developed a generalized nonequilibrium DMFT formalism to study the response of correlated electrons to a spatially uniform time-dependent electric field and applied that formalism

to the Falicov-Kimball model.[6–8] The Falicov-Kimball model,[21] is the simplest model for strongly correlated electrons that demonstrates long range order and undergoes a metal-to-Mott-insulator transition. It consists of two kinds of electrons: conducting $c$-electrons and localized $f$-electrons, which interact through an on-site Coulomb repulsion. The model was introduced to describe valence-change and metal-insulator transitions[21] in rare-earth and transition-metal compounds. It was reinvented as a model to describe crystal formation[22] resulting from the Pauli exclusion principle. DMFT was actually developed with the original solution of the Falicov-Kimball model in infinite dimensions[1,10,11] and now there is an almost complete understanding of its general properties (for a review, see Ref. 19). We extended the equilibrium formalism to the nonequilibrium case, where we numerically solved a system of the equations for the Green function and self-energy defined on a complex time contour (see Fig. 1.1) by using the Kadanoff-Baym-Keldysh nonequilibrium Green function formalism.[23,24]

In this review, we summarize the successes of recent work to generalize DMFT to nonequilibrium problems with a focus on solutions of the spinless Falicov-Kimball model on an infinite-dimensional hypercubic lattice in the presence of an external time-dependent electric field. There are many interesting and surprising results which differ from semiclassical predictions (such as those made from the Boltzmann equation solution). In addition to the exact solutions, we also present results for the noninteracting case and for the case of second-order perturbation theory in the interaction. In particular, we analyze the limitations of the perturbation theory approximation, especially in studying (long-time) steady-state behavior.

### 1.2. General nonequilibrium formalism

The nonequilibrium properties of a quantum many-particle system can be studied by calculating the contour-ordered Green function in momentum space:

$$\begin{aligned} G^c_{\mathbf{k}}(t_1,t_2) &= -i\langle \hat{\mathrm{T}}_c c_{\mathbf{k}H}(t_1) c^\dagger_{\mathbf{k}H}(t_2)\rangle \\ &= \frac{-i\mathrm{Tr}\left\{e^{-\beta H(-t_{\max})}\hat{\mathrm{T}}_{\mathrm{c}} \exp[-i\int_c dt H_I(t)] c_{\mathbf{k}I}(t_1) c^\dagger_{\mathbf{k}I}(t_2)\right\}}{\mathrm{Tr}e^{-\beta H(-t_{\max})}}, \end{aligned} \quad (1.1)$$

defined on the complex time-contour presented in Fig. 1.1 (see, for example, Ref. 25). Since the system is initially in equilibrium, the thermal average in Eq. (1.1) is performed with the equilibrium density matrix

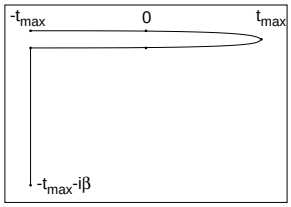


Fig. 1.1. The complex Kadanoff-Baym-Keldysh time contour for the two-time Green functions in the nonequilibrium case. The time increases from $-t_{max}$ (left point on the top branch) along the contour to $t_{max}$ then decreases back to $-t_{max}$ and then runs parallel to the imaginary axis to $-t_{max} - i\beta$. We consider the situation when the electric field is turned on at $t = 0$, so the vector potential is nonzero for $t > 0$. We assume that both $t_1$ and $t_2$ lie somewhere on the contour.

$\exp[-\beta H(-t_{\rm max})]/{\rm Tr}\exp[-\beta H(-t_{\rm max})]$ with respect to the initial Hamiltonian $H(-t_{\rm max})$ with vanishing electric field (the symbol $\beta = 1/T$ is the inverse temperature). The operator indices $H$ and $I$ in Eq. (1.1) stand for the Heisenberg and Interaction representations, respectively. In this formalism, familiar quantum many-body techniques derived in equilibrium can also be used in the nonequilibrium case, except that now the time ordering $\hat{\rm T}_{\rm c}$ of the operators is along the complex contour. In particular, the Schwinger-Dyson equation, which connects the contour-ordered Green function with the electron self-energy $\Sigma^c_{\mathbf{k}}(t_1, t_2)$, remains valid:

$$G^c_{\mathbf{k}}(t_1, t_2) = G^{0c}_{\mathbf{k}}(t_1, t_2) + \int_c dt \int_c d\bar{t} G^{0c}_{\mathbf{k}}(t_1, t)\Sigma^c_{\mathbf{k}}(t, \bar{t})G^c_{\mathbf{k}}(\bar{t}, t_2), \qquad (1.2)$$

where the matrix product of the continuous matrix operators is accomplished by line integrals over the contour.

In DMFT, we work with the local Green function, which is found by summing the momentum-dependent Green function over all momenta. We then map the many-body problem on the lattice to an impurity problem, but in a dynamical mean field that mimics the hopping of electrons onto and off of the given site. It turns out that one needs the full freedom available with the three-branch contour to find the proper dynamical mean field to map the impurity onto the lattice. Hence, our approach will work with the less common Green functions on the three-branch contour, as opposed to a simpler two-branch contour, which we work with when we discuss the perturbative approach on the lattice. One can find the time-ordered, anti-time-ordered, lesser, greater, retarded, advanced and thermal Green functions on this contour.[26] For example, the retarded Green function,

which is related to the density of quantum states, is

$$G^R_{\mathbf{k}}(t_1,t_2) = -i\theta(t_1-t_2)\langle\{c_{\mathbf{k}H}(t_1), c^\dagger_{\mathbf{k}H}(t_2)\}_+\rangle, \tag{1.3}$$

where the braces indicate the anticommutator of the two operators, and the lesser Green function, which is related to how the electrons are distributed amongst the quantum states, satisfies

$$G^<_{\mathbf{k}}(t_1,t_2) = i\langle c^\dagger_{\mathbf{k}H}(t_2)c_{\mathbf{k}H}(t_1)\rangle. \tag{1.4}$$

Both of these functions can be extracted from $G^c_{\mathbf{k}}$.

## 1.3. Nonequilibrium dynamical mean-field theory for the Falicov-Kimball model

The spinless Falicov-Kimball model[21] consists of two kinds of electrons: conduction $c$-electrons and localized $f$-electrons. They interact with each other through an on-site Coulomb repulsion $U$. The model Hamiltonian has the following form in the absence of any external fields:

$$\mathcal{H} = -\sum_{\langle ij\rangle} t_{ij}c^\dagger_i c_j - \mu\sum_i c^\dagger_i c_i - \mu_f\sum_i f^\dagger_i f_i + U\sum_i f^\dagger_i f_i c^\dagger_i c_i, \tag{1.5}$$

where $t_{ij} = t$ is the nearest-neighbor hopping matrix element for the $c$-electrons, $\mu$ and $\mu_f$ are the chemical potentials of $c$- and $f$-electrons, correspondingly. Due to the Pauli principle, there is no local $cc$- and $ff$-electron interaction in the spinless case. The Hamiltonian in Eq. (1.5) can also be regarded as an approximation to the spin $s = 1/2$ Hubbard model, where spin-up ($c$-) electrons move in a frozen background of the localized spin-down ($f$-electrons). We consider the problem on the infinite-dimensional ($d \to \infty$) hypercubic lattice at half-filling, when the particle densities of the $c$- and $f$-electrons are equal to 0.5. In this limit, the hopping parameter is renormalized in the following way:[2] $t = t^*/2\sqrt{d}$. In the limit of infinite dimensions, one can solve the equilibrium problem for the conduction electrons exactly at any temperature, particle concentration and Coulomb repulsion. The key simplification, which allows one to obtain the exact solution as $d \to \infty$, comes from the fact that the electron self-energy is momentum-independent.[1,27] Although that original work was performed in equilibrium, Langreth's rules[28] guarantee that it also holds for the nonequilibrium case.

Nowadays, most of the equilibrium properties of the model, including the phase diagram, are well known (see Ref. 19). In particular, the model

demonstrates a Mott transition when $n_c + n_f = 1$ at some critical value of the Coulomb repulsion,[29] which depends on the particular value of $n_c$ ($n_f$ is equal to $1 - n_c$ in this case). In the insulating phase, the density of states $A(\omega)$ is not equal to zero for frequencies inside the "gap region", but is exponentially suppressed, except for $\omega = 0$. Therefore, the density of states actually demonstrates a pseudogap in the insulating phase, which is an artifact of the fact that the infinite-dimensional hypercubic lattice has a Gaussian density of states for the noninteracting problem, which does not have a finite bandwidth. Another important feature is the behavior of the imaginary part of the self-energy for frequencies close to zero in the "metallic" phase: $\mathrm{Im}\Sigma(\omega) \sim -c + c'\omega^2$ ($c$ and $c' > 0$ and independent of temperature), which differs from the standard Fermi liquid behavior $\mathrm{Im}\Sigma(\omega) \sim -a(T) - b\omega^2$ ($a$ and $b > 0$ and $a(T) \to 0$ as $T \to 0$). This means that there are no long-lived Fermi liquid quasiparticles in the model.

We are interested in the case when the system is coupled to an external electromagnetic field $\mathbf{E}(\mathbf{r}, t)$. This field can be expressed by a scalar potential $\varphi(\mathbf{r}, t)$ and by a vector potential $\mathbf{A}(\mathbf{r}, t)$ in the following way:

$$\mathbf{E}(\mathbf{r}, t) = -\nabla\varphi(\mathbf{r}, t) - \frac{1}{c}\frac{\partial \mathbf{A}(\mathbf{r}, t)}{\partial t}. \tag{1.6}$$

We assume that the electric field is spatially uniform and choose the temporal or Hamiltonian gauge for the electric field: $\varphi(\mathbf{r}, t) = 0$. In this case, the electric field is introduced into the Hamiltonian by means of the Peierls substitution for the hopping matrix:[30]

$$t_{ij} \to t_{ij} \exp\left[-\frac{ie}{\hbar c}\int_{\mathbf{R}_i}^{\mathbf{R}_j} \mathbf{A}(\mathbf{r}, t) d\mathbf{r}\right] = t_{ij} \exp\left[\frac{ie}{\hbar c}\mathbf{A}(t) \cdot (\mathbf{R}_i - \mathbf{R}_j).\right], \tag{1.7}$$

where the last formula holds for a spatially uniform field where we take $\mathbf{A}(t) = -\mathbf{E}ct\theta(t)$ for a uniform field turned on at $t = 0$.

We assume that it is safe to neglect magnetic field effects, because the electric field varies slow enough in time (recall Maxwell's equations say that a time-varying electric field creates a time varying magnetic field). This approximation is valid when the electric field is smooth enough in time that the magnetic fields can be ignored. Another way of describing this is that we assume our electric field is always spatially uniform, even though it has a time dependence, which is not precisely a solution of Maxwell's equations, but is approximately so.

The electric field introduced into the Hamiltonian Eq. (1.5) results in a time-dependent shift of the momentum in the free electron dispersion

relation:

$$\epsilon\left(\mathbf{k}-\frac{e\mathbf{A}(t)}{\hbar c}\right)=-2t\sum_{l=1}^{d}\cos\left[a\left(k^{l}-\frac{eA^{l}(t)}{\hbar c}\right)\right]. \tag{1.8}$$

It is convenient to consider the case, when the electric field lies along the elementary cell diagonal:[31]

$$\mathbf{A}(t)=A(t)(1,1,...,1). \tag{1.9}$$

In this case, the free electron spectrum

$$\epsilon\left(\mathbf{k}-\frac{e\mathbf{A}(t)}{\hbar c}\right)=\cos\left(\frac{eaA(t)}{\hbar c}\right)\epsilon(\mathbf{k})+\sin\left(\frac{eaA(t)}{\hbar c}\right)\bar{\varepsilon}(\mathbf{k}), \tag{1.10}$$

depends on only two energy functions:

$$\epsilon(\mathbf{k})=-2t\sum_{l}\cos(ak^{l}) \tag{1.11}$$

and

$$\bar{\varepsilon}(\mathbf{k})=-2t\sum_{l}\sin(ak^{l}). \tag{1.12}$$

Of course, when the field vanishes, the energy spectra in Eq. (1.10) reduces to the standard spectra in Eq. (1.11) for free electrons on the hypercubic lattice. In the limit of an infinite dimensional hypercubic lattice, one can calculate the joint density of states for the two energy functions in Eqs. (1.11) and (1.12),[32]

$$\rho_{2}(\epsilon,\bar{\varepsilon})=\frac{1}{\pi t^{*2}a^{d}}\exp\left[-\frac{\epsilon^{2}}{t^{*2}}-\frac{\bar{\varepsilon}^{2}}{t^{*2}}\right]. \tag{1.13}$$

Below we use atomic units, putting all fundamental constants, except the electron charge $e$, to be equal to one: $a=\hbar=c=t^{*}=1$.

To solve the problem of the response of the conduction electrons to an external electric field, we use a generalized nonequilibrium DMFT formalism.[8] The electron Green functions and self-energies are functions of two time arguments defined on the complex time-contour in Fig. 1.1. Since the action for the Falicov-Kimball model is quadratic in the conduction electrons, the Feynman path integral over the Kadanoff-Baym-Keldysh contour can be expressed by the determinant of a continuous matrix operator with arguments defined on the contour. Because the concentration of localized particles on each site is conserved, one can calculate the trace over the fermionic variables. It is possible to show that the self-energy remains local in the limit of infinite dimensions in the presence of a field; start with the

equilibrium perturbation theory expansion for the self-energy[27] and then apply Langreth's rules[28] to the self-energy diagrams, which say that every nonequilibrium diagram is obtained from a corresponding equilibrium diagram, with the time variables now defined on the Kadanoff-Baym-Keldysh contour.

The generalized system of nonequilibrium DMFT equations for the contour ordered Green function $G(t_1,t_2)$, self-energy $\Sigma(t_1,t_2)$ and an effective dynamical mean-field $\lambda(t_1,t_2)$ can be written in analogy with the equilibrium case[12] as follows:

$$G(t_1,t_2) = \sum_{\mathbf{k}} [G_{\mathbf{k}}^{(0)-1} - \Sigma]^{-1}(t_1,t_2), \tag{1.14}$$

$$G_0(t_1,t_2) = [G^{-1} + \Sigma]^{-1}(t_1,t_2), \tag{1.15}$$

$$\lambda(t_1,t_2) = G_{0imp}^{-1}(t_1,t_2;\mu) - G_0^{-1}(t_1,t_2), \tag{1.16}$$

$$G(t_1,t_2) = (1-w_1)G_0(t_1,t_2) + w_1[G_{0imp}^{-1}(\mu - U) - \lambda]^{-1}(t_1,t_2) \tag{1.17}$$

where $G_{\mathbf{k}}^{(0)}(t_1,t_2)$ is the noninteracting electron Green function in the presence of an external time-dependent electric field, which can be calculated analytically (see below) and $G_{0imp}(t_1,t_2;\mu)$ is the free impurity Green function in a chemical potential $\mu$. The symbol $w_1$ is the average number of the $f$-electrons per site. In our case, $w_1 = 1/2$.

The momentum summation in Eq. (1.14) can be performed by introducing the two energy functions Eqs. (1.11) and (1.12) and using the joint density of states in Eq. (1.13): $\sum_{\mathbf{k}} F_{\mathbf{k}} = \int d\epsilon \int d\bar{\varepsilon} \rho_2(\epsilon,\bar{\varepsilon}) F_{\epsilon,\bar{\varepsilon}}$ whenever the summand $F_{\mathbf{k}}$ depends on momentum only through the two energy functions. The system of equations (1.14)-(1.17) formally resembles the corresponding system in the equilibrium case, except now we have to work with a two-time formalism on the contour, rather than being able to Fourier transform the relative time to a frequency. And, because we are working with the contour-ordered Green functions, which depend on the distribution of electrons, we need to be careful to treat how the chemical potential is shifted by $U$ when we perform the trace over the $f$-electrons.

The system of equations (1.14)-(1.17) can be solved by iteration as follows. One starts with an initial self-energy matrix, for example the equilibrium self-energy. Substitution of this function into Eq. (1.14) gives the Green function. Then, from Eq. (1.16) one can find the effective dynamical mean-field $\lambda(t_1,t_2)$, which allows one to find the new value for the Green function $G(t_1,t_2)$ from Eq. (1.17). After that, one finds the new self-energy $\Sigma(t_1,t_2)$ from the impurity Dyson equation and the dynamical mean field.

The calculations are repeated until the difference between the old and new values for the self-energy $\Sigma(t_1, t_2)$ are smaller than some desired precision (usually $10^{-6}$ in relative error).

In practice, to solve this system numerically, one needs to discretize the complex time contour Fig. (1.1) with some step $\Delta t$ along the real axis and $\Delta\tau$ along the imaginary axis. In this case, the functions in Eqs. (1.14)-(1.17) become general complex square matrices. In order to study the long time behavior, one needs to choose the value of $t_{max}$ large enough. The precision of the solution strongly depends on the value of the discretization step $\Delta t$, which must be small enough. Therefore, in order to get a precise long time solution it is necessary to use large complex square matrices in Eqs. (1.14)-(1.17). This causes some constraints connected with the machine memory and the computational time. In our calculations, we used the time step $\Delta t$ ranging from 0.1 to 0.0167 and matrices up to order $4900 \times 4900$. The two-energy integration in Eq. (1.14) was performed by using a Gaussian integration scheme (for details, see Ref. 6). Since each energy is independent of each other, the algorithm parallelizes naturally.

It is important to find ways to benchmark this nonequilibrium DMFT algorithm, to ensure that it is accurate. The simplest way to do this is to calculate the equilibrium results within the nonequilibrium formalism and compare those results with the results obtained by the equilibrium DMFT approach. One of the most important elements is a proper choice of the discretization step $\Delta t$ of the contour. These equilibrium calculations can always help to choose the step $\Delta t$ small enough to get correct results (see Ref. 6). Another useful way to check the accuracy of the solution is to calculate the moments of the electron spectral functions $A(t_{ave}, \omega) = \sum_{\mathbf{k}}(-1/\pi)\mathrm{Im}G_{\mathbf{k}}(t_{ave}, \omega)$, where $t_{ave}$ is the average time and $\omega$ is the electron frequency arising from a Fourier transform of the relative time (see below). We have found[7] that the lowest spectral moments in the Falicov-Kimball model can be calculated exactly, and they are time-independent even in the presence of a time-dependent electric field. In particular, when a spatially homogeneous time-dependent electric field is applied, one can find for the zeroth and first two retarded spectral moments:

$$\int_{-\infty}^{\infty} d\omega A^R(t_{ave}, \omega) = 1, \tag{1.18}$$

$$\int_{-\infty}^{\infty} d\omega\omega A^R(t_{ave}, \omega) = -\mu + Un_f = 0, \tag{1.19}$$

$$\int_{-\infty}^{\infty} d\omega \omega^2 A^R(t_{ave},\omega) = \frac{1}{2} + \mu^2 - 2U\mu n_f + U^2 n_f = \frac{1}{2} + \frac{U^2}{4}, \quad (1.20)$$

where the second equality holds in the half-filled case. We estimate the accuracy of the discretization of the contour by calculating the spectral moments and comparing them with the exact analytical results in Eqs. (1.18)-(1.20).[7] In general, one needs to reduce the discretization size as the interaction strength increases. This is clearly seen in the equilibrium case, where the numerics can be well controlled because there is no dependence on the energy $\bar{\varepsilon}$. Surprisingly, in the presence of a field, one can use a somewhat larger discretization size, especially for moderate to large fields.

### 1.4. Gauge invariance and physical observables

In nonequilibrium problems, we work with two-time Green functions because the system no longer has time-translation invariance. Wigner[33] first realized that it is more physical to express results in terms of average and relative coordinates, where the dependence on the average coordinates drops out in equilibrium. In our case, the relative and average times satisfy

$$t = t_1 - t_2, \quad t_{ave} = \frac{t_1 + t_2}{2} \quad (1.21)$$

while for the spatial coordinates we have

$$\mathbf{r} = \mathbf{r}_1 - \mathbf{r}_2, \quad \mathbf{r}_{ave} = \frac{\mathbf{r}_1 + \mathbf{r}_2}{2}; \quad (1.22)$$

note that at this point we are restricting the time coordinates to lie on the real axis piece of the contour since the imaginary axis piece is not important for determining physical properties on the lattice (the full structure is only needed for the self-consistent DMFT loop, not for calculating any physical properties once the self-energy has been determined). We want to be able to convert the relative time and space coordinates into frequency and momentum via a Fourier transformation. Since we are working with a uniform electric field, we expect that the system will have no average spatial coordinate dependence, because it is spatially homogeneous. The easiest way to construct the right transformation is to create a Fourier transformation that makes the gauge-invariance of the problem manifest; the result is then called the gauge-invariant Green function, which depends only on the fields, not on the scalar or vector potentials.[5] The procedure is somewhat technical, but completely straightforward. The starting point

is a generalized Fourier transformation

$$G(\mathbf{k},\omega,\mathbf{r}_{ave},t_{ave}) = \int d^d r \int dt \exp[iW(\mathbf{k},\omega,\mathbf{r},t,\mathbf{r}_{ave},t_{ave})] \times G(\mathbf{r},t,\mathbf{r}_{ave},t_{ave}), \quad (1.23)$$

with $W$ being a complicated function of its variables, in general. In equilibrium, when there is no external space- and time-dependent electric field, the Green function doesn't depend on the average coordinates $t_{ave}$ and $\mathbf{r}_{ave}$, and the transform (1.23) is the well-known Fourier transformation with $W(\mathbf{k},\omega,\mathbf{r},t,\mathbf{r}_{ave},t_{ave}) = t\omega - \mathbf{r}\cdot\mathbf{k}$.

The situation is more complicated when an external field is present. In this case, the field is introduced by using a specific gauge for the scalar and vector potential (we work with the Hamiltonian gauge). It is important to have a Green function on the left hand side of Eq. (1.23), which doesn't depend on the choice of gauge so all results are manifestly independent of the scalar and vector potentials. Therefore, we need to construct a function $W(\mathbf{k},\omega,\mathbf{r},t,\mathbf{r}_{ave},t_{ave})$ in Eq. (1.23), which makes $G(\mathbf{k},\omega,\mathbf{r}_{ave},t_{ave})$ invariant under the gauge transformation:

$$\varphi(\mathbf{r}_1,t_1) \to \varphi(\mathbf{r}_1,t_1) - \frac{\partial\chi(\mathbf{r}_1,t_1)}{\partial t_1}, \quad (1.24)$$

$$\mathbf{A}(\mathbf{r}_1,t_1) \to \mathbf{A}(\mathbf{r}_1,t_1) + \nabla\chi(\mathbf{r}_1,t_1), \quad (1.25)$$

where $\chi(\mathbf{r}_1,t_1)$ is an arbitrary function. The $\chi$ function must also be used in the local unitary gauge transformation of the fermion operators:

$$c(\mathbf{r}_1,t_1) \to \exp[ie\chi(\mathbf{r}_1,t_1)]c(\mathbf{r}_1,t_1), \quad (1.26)$$

$$c^\dagger(\mathbf{r}_2,t_2) \to \exp[-ie\chi(\mathbf{r}_2,t_2)]c^\dagger(\mathbf{r}_2,t_2), \quad (1.27)$$

since it corresponds to the phase picked up by the fermions as a result of the local gauge transformation. Obviously, the Green function on the right hand side of Eq. (1.23) is not generically invariant in this case:

$$G(\mathbf{r}_1,t_1;\mathbf{r}_2,t_2) \to \exp[ie(\chi(\mathbf{r}_1,t_1) - \chi(\mathbf{r}_2,t_2))]G(\mathbf{r}_1,t_1;\mathbf{r}_2,t_2). \quad (1.28)$$

However, it is possible to show that its transform in Eq. (1.23) is invariant, when one chooses[5]

$$W(\mathbf{k},\omega,\mathbf{r},t,\mathbf{r}_{ave},t_{ave}) = \int_{-1/2}^{1/2} d\lambda\{t[\omega + e\varphi(\mathbf{r}_{ave}+\lambda\mathbf{r},t_{ave}+\lambda t)) - \mathbf{r}\cdot(\mathbf{k}+e\mathbf{A}(\mathbf{r}_{ave}+\lambda\mathbf{r},t_{ave}+\lambda t)]\} \quad (1.29)$$

(for details, see Ref. 34).

In the case of a spatially homogeneous electric field in the Hamiltonian gauge with $\varphi(\mathbf{r},t)=0$, which we study in this paper, this transformation is

$$\tilde{G}(\mathbf{k},t,\mathbf{r}_{ave},t_{ave}) \to G\left(\mathbf{k}-\frac{1}{t}\int_{-t/2}^{t/2} e\mathbf{A}(t_{ave}+\bar{t})d\bar{t},t,\mathbf{r}_{ave},t_{ave}\right), \quad (1.30)$$

because the function $W$ just involves a shift of the momentum; note that the Green function is actually independent of $\mathbf{r}_{ave}$ in this case. Hence, the gauge invariant Green function in the momentum representation contains a shift of the momentum, which depends on both the relative and average time coordinates. We consider the case when a constant electric field is turned on at time $t=0$: $\mathbf{A}(t)=-\mathbf{E}t\theta(t)$. Then the momentum shift is

$$\begin{aligned}\mathbf{k}\to\mathbf{k}-e\mathbf{E}\Big[&t_{ave}\theta(t_{ave}-|t/2|)\\&+\left(-\frac{t_{ave}^2}{2t}+\frac{t_{ave}}{2}-\frac{t}{8}\right)\theta(-t/2-|t_{ave}|)\\&+\left(\frac{t_{ave}^2}{2t}+\frac{t_{ave}}{2}+\frac{t}{8}\right)\theta(t/2-|t_{ave}|)\Big].\end{aligned} \quad (1.31)$$

Note that this shift does not depend on the relative time coordinate $t$ for long times, $t_{ave}>|t/2|$. However, in general, one has to first shift the momentum, and then Fourier transform the relative time to a frequency. It is important that the time-dependent momentum shift takes place for some negative average times (if the absolute value of the relative time is large enough, then either $t_1$ or $t_2$ is larger than 0 and hence "sees" the field).

The shift of the momentum becomes particularly simple for equal time Green functions, such as those needed to calculate the current flowing or to determine the distribution of the electrons amongst the quantum states. In this case, $t=0$, and the momentum is shifted by $-e\mathbf{E}t_{ave}$ if $t_{ave}>0$. Therefore, gauge invariant Green functions can be obtained from the Hamiltonian gauge Green functions by simply shifting the momentum by $-e\mathbf{E}t_{ave}$. Note that local quantities, like the local density of states or the local distribution function are always gauge invariant, because they are summed over momentum, and if the shift is the same for each momentum value, then we still sum over all the momentum points in the Brillouin zone. In cases where the relative time is nonzero, the transformation from the Green function in a particular gauge to the gauge-invariant Green function must be handled with care. Finally, one should note that in the steady state, where $t_{ave}\to\infty$, the momentum shift is also simple ($-e\mathbf{E}t_{ave}$); it turns out

that the retarded and advanced Green functions depend only on the relative time, but the lesser, greater, and Keldysh Green functions depend on both the average and relative time because there is an average-time-dependent shift of the momentum in Fermi-Dirac distribution functions. Caution must be used in trying to directly find the steady-state Green functions, because the Dyson equation is modified, since the momentum shift does not remove all average time dependence in internal variables that are integrated over in the $G_0 \Sigma G$ term.

### 1.5. Bloch electrons in infinite dimensions

The work presented in this section is based on Ref. 31 where the original solution for Bloch electrons in a field was given. There the work focused on the Hamiltonian gauge, here we discuss the gauge-invariant formalism.

Bloch[35] and Zener[36] originally showed that when electrons are placed on a perfect lattice, with no scattering, the current oscillates due to Bragg reflection of the wavevector as it evolves to the Brillouin-zone boundary. Here we show how to analyze this problem on the infinite-dimensional hypercubic lattice. The noninteracting problem can be solved exactly in the case of an arbitrary time-dependent electric field. In particular, the noninteracting contour-ordered Green function is (in the Hamiltonian gauge[31]):

$$\begin{aligned} G^{c0}_{\mathbf{k}}(t_1,t_2) = \quad & i[f(\epsilon(\mathbf{k})-\mu)-\theta_c(t_1,t_2)]\exp[i\mu(t_1-t_2)] \\ & \times \exp\left[-i\int_{t_2}^{t_1} d\bar{t}\epsilon\left(\mathbf{k}-e\mathbf{A}(\bar{t})\right)\right], \end{aligned} \tag{1.32}$$

where $f(\epsilon(\mathbf{k})-\mu)] = 1/\{1+\exp[\beta(\epsilon(\mathbf{k})-\mu)]\}$ is the Fermi-Dirac distribution (half-filling corresponds to $\mu = 0$). The symbol $\theta_c(t_1,t_2)$ is equal to one if $t_1$ lies after $t_2$ on the contour, and is zero otherwise. Note that the Green function in Eq. (1.32) is also used in the system of equations (1.14)-(1.17) to solve the interacting problem.

When we have a constant electric field directed along the diagonal and turned on at $t = 0$, each component of the vector potential satisfies $A(t) =$

$-Et\theta(t)$. Then the integral that appears in the exponent of Eq. (1.32) is

$$\begin{aligned}
&\theta(-|t/2|-t_{ave})\epsilon(\mathbf{k})t \qquad (1.33)\\
&+\theta(-t/2-|t_{ave}|)\\
&\times\left[\frac{\epsilon(\mathbf{k})(\sin eE(t_{ave}-t/2)+t_{ave}+t/2)-\bar{\varepsilon}(\mathbf{k})(\cos eE(t_{ave}-t/2)-1)}{eE}\right]\\
&+\theta(t/2-|t_{ave}|)\\
&\times\left[\frac{\epsilon(\mathbf{k})(\sin eE(t_{ave}+t/2)-t_{ave}+t/2)+\bar{\varepsilon}(\mathbf{k})(\cos eE(t_{ave}+t/2)-1)}{eE}\right]\\
&+\theta(t_{ave}-|t/2|)\Big[\epsilon(\mathbf{k})(\sin eE(t_{ave}+t/2)\\
&\quad-\sin eE(t_{ave}-t/2))+\bar{\varepsilon}(\mathbf{k})(\cos eE(t_{ave}+t/2)-\cos eE(t_{ave}-t/2))\Big]\Big/eE
\end{aligned}$$

when expressed in terms of the Wigner coordinates.

To get the gauge-invariant Green function, we now shift the momentum as shown in Eq. (1.31); note that the shift is done both for the momentum in the exponent, and for the momentum in the Fermi-Dirac distribution. Two of the four cases for the exponent in Eq. (1.33) are easy to work out for the gauge-invariant Green functions. The first is the $\theta(-|t/2|-t_{ave})$ term which remains unchanged and the second is the $\theta(-t/2-|t_{ave}|)$ term, which becomes $2\epsilon(\mathbf{k})\sin(eEt/2)$. Note that both these exponents are independent of the average time. The average time enters for the other two terms, and in the argument of the Fermi-Dirac distribution.

The retarded $G^{R0}_{\mathbf{k}}(t_1,t_2)$ and lesser $G^{<0}_{\mathbf{k}}(t_1,t_2)$ Green functions can be obtained from Eq. (1.32), by replacing the prefactor $[f(\epsilon(\mathbf{k})-\mu)-\theta_c(t_1,t_2)]$ by $-i\theta(t_1-t_2)$ and $f(\epsilon(\mathbf{k})-\mu)$, correspondingly. One needs to shift the momentum accordingly to get the gauge-invariant retarded and lesser Green functions. Note that at long times the gauge-invariant retarded Green function depends only on relative time.

Since the electrical current is found from the time derivative of the polarization operator, the current operator is determined by taking the commutator of the Hamiltonian (in a particular gauge) with the polarization operator. The result, for the $\alpha$th component of the current-density operator is

$$\mathbf{j}_\alpha(t_{ave})=e\sum_{\mathbf{k}}\frac{\partial\epsilon(\mathbf{k}-e\mathbf{A}(t_{ave}))}{\partial k_\alpha}c^\dagger_{\mathbf{k}}(t_{ave})c_{\mathbf{k}}(t_{ave}), \qquad (1.34)$$

where we have emphasized that the operator is evaluated with a vanishing relative time ($t=0$). We want the expectation value of the current

operator, which is found by taking expectation value of the expression in Eq. (1.34) and noting that each component gives the same result for a field pointing along the diagonal. The expectation value of the product $c^\dagger_{\mathbf{k}}(t_{ave})c_{\mathbf{k}}(t_{ave})$ can be replaced by the lesser Green function $G^<_{\mathbf{k}}(t_{ave},0)$. So we have

$$j(t_{ave}) = ie\sum_{\mathbf{k}} \bar{\varepsilon}\left(\mathbf{k} - e\mathbf{A}(t_{ave})\right) G^<_{\mathbf{k}}(t_{ave},0) = ie\sum_{\mathbf{k}} \bar{\varepsilon}\left(\mathbf{k}\right) \tilde{G}^<_{\mathbf{k}}(t_{ave},0), \tag{1.35}$$

where the second equality comes from the transformation to the gauge-invariant Green function. The summation over momentum can be converted to a double integral over the joint density of states in Eq. (1.13). Substituting in the expression for the lesser Green function, yields

$$j(t_{ave}) = \frac{et^*}{4\sqrt{d}\pi}\sin(eEt_{ave})\int d\epsilon \frac{df(\epsilon-\mu)}{d\epsilon}\rho(\epsilon), \tag{1.36}$$

where the single-particle density of states is

$$\rho(\epsilon) = \int d\bar{\varepsilon}\rho_2(\epsilon,\bar{\varepsilon}) = \frac{1}{\sqrt{\pi}}\exp\left[-\epsilon^2\right]. \tag{1.37}$$

The current is a periodic function of time, even though the field is time-independent; this effect is called a Bloch oscillation.[37] The period of the oscillation is equal to $2\pi/eE$. In order to see this oscillation in real solids, one needs to prepare a system where the scattering time is longer than the period of the Bloch oscillations. In solids, the scattering time is much shorter than the oscillation period, so this effect is not observed. However, Bloch oscillations are seen in semiconductor superlattices, where the period of oscillations is much shorter due to the larger lattice spacing. As we show in the following Sections, the effects of strong electron-electron correlations modify the Bloch oscillations significantly, but the driven oscillations in large fields survive for a surprisingly long time.

Now we discuss the time-dependence of the density of states (DOS) for noninteracting electrons in a constant electric field. The DOS is found by using the Wigner time coordinates in Eq. (1.21), and making a Fourier transformation of the corresponding Green functions with respect to the relative time coordinate. In particular, the local DOS is

$$A(t_{ave},\omega) = -\frac{1}{\pi}\mathrm{Im}\int_0^\infty dt e^{i\omega t} G^R_{loc}(t_{ave},t). \tag{1.38}$$

Since this is a local quantity, summed over all momenta, it is automatically gauge-invariant. The local retarded Green function can be obtained from

Eq. (1.32). It is possible to show[31] that the steady state ($t_{ave} \to \infty$), for the case of a constant electric field turned on at $t = 0$, has a retarded Green function which satisfies

$$G^R_{loc}(t_{ave} \to \infty, t) = -i\theta(t) \exp\left[\frac{1}{2e^2E^2}\left\{\cos(eEt) - 1\right\}\right]. \qquad (1.39)$$

Substitution of this expression into Eq. (1.38), and evaluating the Fourier transform with respect to the relative time, yields the steady state DOS, which consists of a set of delta-functions with different amplitudes (called the Wannier-Stark ladder[38]). The distance between the delta-function peaks is equal to $eE$. The weight of these peaks is:[31]

$$w_N = \frac{2}{e^2E^2}\int_0^{2\pi} du \cos(Nu) \exp(\frac{t^{*2}}{2e^2E^2}[\cos u - 1]), \qquad (1.40)$$

for the $N$th Bloch frequency, $\omega_N = eEN$. It takes an infinite amount of time for the delta functions to develop.

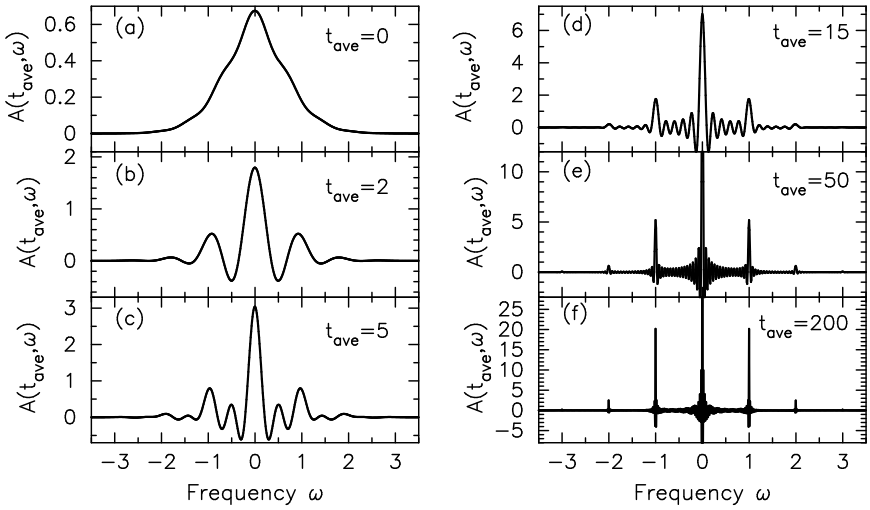


Fig. 1.2. Density of states for noninteracting electrons with $eE = 1$ at different values of time $t_{ave}$ (be aware that the vertical scale changes from plot to plot). Note how the build up of the delta function at the Bloch frequencies is slow.

In Fig. 1.2, we show how the DOS evolves from the time the field is turned on, at $t_{ave} = 0$, to a large time. The DOS remains Gaussian for $t_{ave} < -2$ and then develops large oscillations as $t_{ave}$ increases. Though the DOS oscillates and acquires negative values in the transient regime, it

is possible to show (numerically) that its first three moments always satisfy the relevant sum rules.

### 1.6. Exact solution

In this Section we present the results for the interacting case,[6,8,9] where we vary the Coulomb repulsion through the metal-insulator transition that occurs at $U_c = \sqrt{2}$. The problem is solved by numerically solving the DMFT loop in Eqs. (1.14)-(1.17).

Once the Green functions and self-energy have been found by self-consistently solving the DMFT equations, we can extract the momentum-dependent lesser Green function and use Eq. (1.35) to find the current. In these calculations, we used the Green functions in a particular gauge, but one could easily shift to the gauge-invariant Green functions if desired. When the field is small, and the correlations are small, we see a damping of the Bloch oscillations, as expected. This is shown in the left panel of Fig. 1.3. One can see that the Bloch oscillations maintain their periodicity, but are damped as the scattering increases. As we start to approach the metal-insulator transition at $U \approx 1.414$, one can see the character of the oscillations start to change. As we move into the insulating phase, as shown in the right panel, the character of the oscillations changes completely, and we no longer see the regular Bloch structure. The oscillations seem to survive to much longer times than would be expected from a Boltzmann equation type of analysis. It remains unclear whether the steady state has some residual oscillations, or it goes to a constant value as predicted by semiclassical ideas.

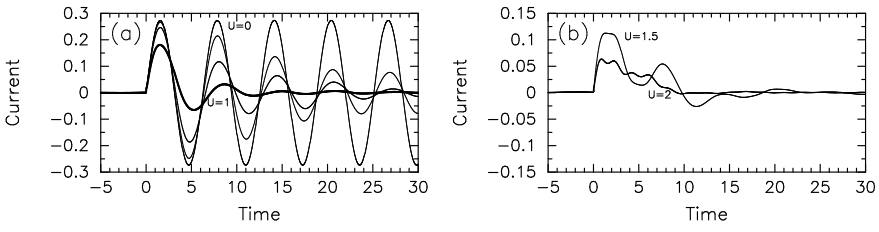


Fig. 1.3. Electric current for different values of $U$ with $\beta = 10$: (a) metals ($U = 0$, $U = 0.25$, $U = 0.5$, and $U = 1$) and (b) insulators ($U = 1.5$ and $U = 2$).

Even more surprising is the fact that when the field is large, the current displays two anomalous features: (i) first, its decay is much slower than ex-

pected from a semiclassical approach, where the relaxation time is inversely proportional to the imaginary part of the self-energy at the chemical potential, which is proportional to $1/U^2$ and (ii) the current develops beats with a beat frequency proportional to $1/U$. An example of this behavior is shown in Fig. 1.4. These beats are always present in the metallic phases (for large $U$), but disappear once one moves into the insulator.

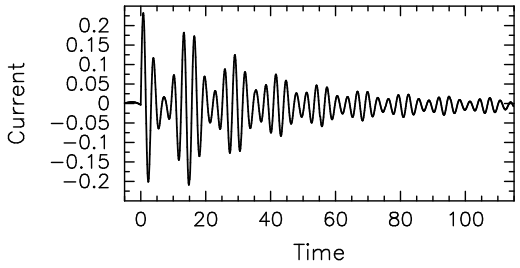


Fig. 1.4. Time-dependence of the current for $U = 0.5$, $E = 2.0$, and $\beta = 10$. Note how the current has beats in its time dependence and that the decay of the current is rather slow.

The time-dependence of the density of states can be calculated from Eq. (1.38). Here, we present some results for the case when the system is initially in the metallic phase, Fig. 1.5. What we find is that for small fields, the delta function peaks of the Wannier-Stark ladder get broadened, but the structure is still readily apparent. But as we increase the field strength, the behavior qualitatively changes, and in the long-time limit, the system evolves into a peaked structure, where the peaks are maximal near the edges of minibands, which are spaced apart in size by $U$, and the DOS has a local minimum in the center, where the Wannier-Stark peak used to appear. This is also behavior that is quite surprising.

As the scattering increases, the DOS approaches the steady state value relatively quickly. This illustrates the dichotomy between the average time, which is important for determining the current, and the relative time, which is important for determining the DOS. The decay is rapid as a function of relative time, but is much slower as a function of average time.

## 1.7. Perturbation theory

A perturbative analysis can be performed directly on the lattice.[40] In this case, we do not need any DMFT loop, and we can restrict the contour to

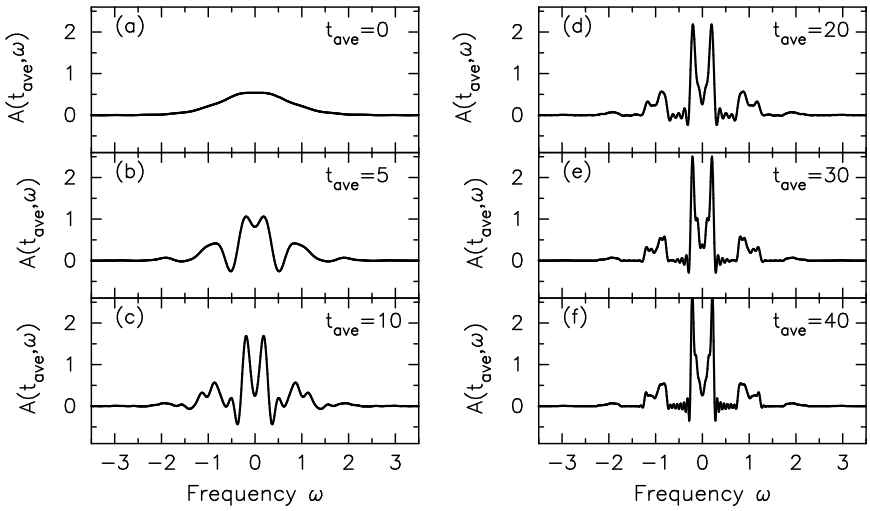


Fig. 1.5. Density of states for different average times from $t_{ave} = 0$ to $t_{ave} = 40$ for $U = 0.5$, $E = 1$ and $\beta = 10$. Note how the DOS develops split peaks, separated by $U = 0.5$ around the Bloch frequencies (integers here)

be solely on the real axis. As described above, the perturbation theory is similar for the equilibrium and nonequilibrium cases, with the only significant changes being that one needs to calculate with time-ordered objects along the contour and one needs to use noninteracting Green functions in the field. A strictly truncated expansion for the self-energy to second order in $U$ is equal to the usual Hartree-Fock term (which vanishes at half filling) plus a second-order term which satisfies

$$\Sigma^{c(2)}(t_1, t_2) = U^2 w_1 (1 - w_1) G^c_{loc}(t_1, t_2); \tag{1.41}$$

one can determine the retarded and lesser self-energies from this in a straightforward fashion. It turns out that this truncated perturbation theory is most accurate at short times—in essence, the perturbation series expansion is an expansion in a power series in time away from the time the field was turned on. In more conventional perturbation series in terms of frequency-dependent Green functions, the perturbation series is most accurate at high frequencies, and least accurate at low frequencies. After performing a Fourier transform, one can immediately see that this is equivalent to the perturbation theory being most accurate at short times and breaking down at long times. Indeed, we find that this perturbative treatment cannot reproduce the steady-state behavior at long times.

As a benchmark of our calculation, we compare the equilibrium self-energy found from a numerical solution of the DMFT equations to the perturbative result for small $U$. We find quite good agreement in the small-$U$ range, and the equilibrium case appears to be fairly accurate up to $U \approx 0.5$. For larger $U$ values the perturbation theory breaks down—it is not capable of properly describing the Mott-insulating phase.

Next we analyze the time-dependence of the electric current calculated by second order perturbation theory in the case when a constant electric field is turned on at time $t = 0$. Before presenting the second-order perturbative solution for the current, we briefly review the corresponding results from a semiclassical Boltzmann equation approximation. As was mentioned above, these results are qualitatively different from the exact solution.

In the Boltzmann equation approach, one introduces a nonequilibrium quasiparticle distribution function $f^{\rm non}(\mathbf{k},t) = -iG^<_{\mathbf{k}}(t,t)$, which satisfies the following phenomenological equation:

$$\frac{\partial f^{\rm non}(\mathbf{k},t)}{\partial t} + e\mathbf{E}(t)\cdot\nabla_{\mathbf{k}} f^{\rm non}(\mathbf{k},t) = -\frac{1}{\tau}[f^{\rm non}(\mathbf{k},t) - f(\mathbf{k})], \tag{1.42}$$

with the boundary condition:

$$f^{\rm non}(\mathbf{k},t=0) = f(\mathbf{k}) = \frac{1}{\exp[\beta(\epsilon(\mathbf{k})-\mu)]+1}. \tag{1.43}$$

This equation can be solved exactly (see, for example Ref. 40). Substitution of the expression for the distribution function instead of $-iG^<$ into Eq. (1.35) allows one to calculate the semiclassical current. This semiclassical current approaches a steady state as time goes to infinity. In particular, in the infinite-dimensional limit one obtains:

$$\begin{aligned} j(t) = -\frac{e}{\sqrt{d}}\frac{eE\tau}{1+e^2E^2\tau^2}\int d\epsilon\rho(\epsilon)\epsilon f(\epsilon) \\ \times\left[1-(\cos(eEt)-eE\tau\sin(eEt))\,e^{-t/\tau}\right]. \end{aligned} \tag{1.44}$$

Therefore, the current is a strongly oscillating function of time for $t \ll \tau$, and it approaches the steady-state value

$$j^{\rm steady} = \frac{eE\tau}{1+e^2E^2\tau^2} j_0, \tag{1.45}$$

where

$$j_0 = -\frac{e}{\sqrt{d}}\int d\epsilon\rho(\epsilon)\epsilon f(\epsilon), \tag{1.46}$$

as $t/\tau \to \infty$. The steady-state current amplitude is proportional to $E$ in the case of a weak field (the linear-response regime), and then becomes

proportional to $1/E$ at $eE\tau \to \infty$. The amplitude of the current goes to zero in this nonlinear regime with the field amplitude increasing. One would naively expect that the second-order perturbation theory would give similar results in the case of a weak Coulomb repulsion, since one can extract an effective scattering time for the equilibrium limit of the Falicov-Kimball model with small $U$: $\tau = 1/(\pi^2 U^2)$.[39] However, it will be shown below, that the behavior of the current calculated in second-order perturbation theory is rather different from the Boltzmann equation case, and closer to the exact numerical result at short times.

The electric current in the second-order perturbation theory can be calculated by substituting the expression for the second-order lesser Green function into Eq. (1.35). In this case

$$j(t) = \frac{ie}{\sqrt{d}} \int d\epsilon \int d\bar{\varepsilon} \rho_2(\epsilon, \bar{\varepsilon}) \left[\bar{\varepsilon} \cos\left(eA_\alpha(t)\right) - \epsilon \sin\left(eA_\alpha(t)\right)\right] G^<_{\epsilon,\bar{\varepsilon}}(t,t). \tag{1.47}$$

It is difficult to find exact analytical expressions for the current, except for some limiting cases. Of course, in the limit $U = 0$ we recover the free electron case result:

$$j(t) = j_0 \sin\left(eEt\right), \tag{1.48}$$

where the amplitude $j_0$ of the Bloch oscillations is given by Eq. (1.46). Therefore, the general expression for the time-dependence of the electric current in a strictly truncated second-order perturbation theory expansion can be written as:

$$j(t) = j_0 \sin\left(eEt\right) + U^2 j_2(t). \tag{1.49}$$

The electric current is a superposition of an oscillating part and some other piece proportional to $U^2$. Obviously this cannot produce a constant steady-state current for all small $U$, because the function $j_2$ is independent of $U$. This is a clear indication that the perturbation theory will hold only for short times.

Numerical results for the time-dependence of the electric current calculated from Eq. (1.47) at $eE = 1$ and different values of $U$ are presented in Fig. 1.6 (dashed lines). Note how the current oscillates for all times within our finite time window. We also show the corresponding Boltzmann equation solution and the exact solution. We use two different values for the Boltzmann equation—one fixes the relaxation time to the prediction from the equilibrium solution, while the other adjusts the relaxation time to obtain the best fit. Comparison of the perturbation theory and the Boltzmann

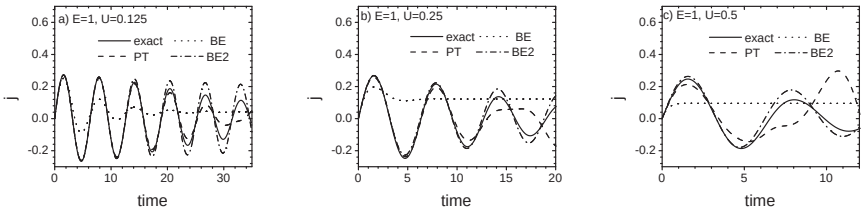


Fig. 1.6. Perturbative expansion for the electric current as a function of time for $E = 1.0$, $\beta = 10$ and different values of $U$ (dashed lines). The solid and dotted lines correspond to the exact DMFT solution and the Boltzmann equation (BE) solution, respectively. The dash-dotted lines (BE2) are the Boltzmann equation result with a phenomenological relaxation time $\tau = \alpha/(\pi^2 U^2)$, while $\alpha = 20$ in Figs. a) and b), and $\alpha = 36.5$ in Fig. c).

equation solution shows that they are close at short times, but at longer times the PT current remains oscillating, while the Boltzmann equation solution approaches a steady state. Moreover, at times longer than $\sim 2/U$ the perturbation theory breaks down showing an oscillating current with increasing amplitude. At times shorter than $2/U$ the perturbation theory solution is close to the exact result, displaying an oscillating current with decreasing amplitude. It is also possible to fit the Boltzmann equation results to the exact and PT solution at short times if one chooses the relaxation time $\tau = \alpha/(\pi^2 U^2)$, where $\alpha \sim 20 - 30$, which is much larger than $\alpha = 1$ in the case of the second order perturbation theory.[39] These results clearly show that the semiclassical approach, with one effective time variable that is damped on the timescale of the relaxation time is not sufficient to describe the behavior in the quantum case.

The perturbation theory calculations at different values of the electric field give results similar to the results presented in Fig. 1.6. Numerical analysis shows that the agreement between the perturbation theory results and the exact results is better when $eE$ is larger than $U$. In fact, it is possible to find an analytical expression for the current in the case of large electric fields:

$$j(t) \simeq -\frac{e}{\sqrt{d}} \int d\epsilon \rho(\epsilon) \epsilon f(\epsilon) \left[1 - U^2 B(\beta) - \frac{U^2}{4} t^2\right] \sin(eEt), \quad (1.50)$$

where $B(\beta)$ is a positive decreasing function of temperature:[40] $0.25 < B(\beta) < 0.5$.

## 1.8. Conclusions

To conclude, we have presented some results on the nonequilibrium properties of the Falicov-Kimball model of strongly correlated electrons in the limit of infinite dimensions. Despite the simplicity of the model, the solutions show that strong electron-electron correlations result in nontrivial behavior. The dynamical mean-field theory approximation is believed to be a precise method to solve strongly correlated problems in three dimensions. Therefore, we believe that some of the results, like the long-time Bloch oscillations of the current, beats in the current for strong fields and the splitting of the Wanier-Stark peaks could be observed in bulk systems with dominant electron-electron scattering in the presence of a strong electric field. Such a field can be present, in particular, in nanostructures, where a moderate external electric potential can produce strong (uniform) electric fields due to the small size of the systems. One might also be able to observe this behavior in mixtures of heavy and light atoms trapped in optical lattices. In addition, we demonstrated that the perturbation theory solution cannot be used to study the long-time behavior of the system. It would be interesting to generalize these results to more complicated models and to lower dimensions, where we expect qualitatively similar behavior.

## Acknowledgments

We thank Antti-Pekka Jauho, Alexander Joura, Joseph Serene and Veljko Zlatić for valuable discussions. We would like to acknowledge support by the National Science Foundation under grant number DMR-0210717 and by the Office of Naval Research under grant number N00014-05-1-0078. Supercomputer time was provided by the DOD HPCMO at the ASC and ERDC centers (including a 2006 CAP project) and by a National Leadership Computing System grant from NASA.

## References

1. U. Brandt and C. Mielsch, Thermodynamics and correlation functions of the Falicov-Kimball model in large dimensions, *Z. Phys. B: Condens. Matter* **75**, 365–370 (1989).
2. W. Metzner and D. Vollhardt, Correlated lattice Fermions in $d = \infty$ dimensions, *Phys. Rev. Lett.* **62**, 324–327 (1989).
3. A. Georges, G. Kotliar, W. Krauth, and M. J. Rozenberg, Dynamical mean-

field theory of strongly correlated fermion systems and the limit of infinite dimensions, *Rev. Mod. Phys.* **68**, 13–125 (1996).
4. G. Kotliar, S. Y. Savrasov, K. Haule, V. S. Oudovenko, O. Parcollet, and C. A. Marianetti, Electronic structure calculations with dynamical mean-field theory, *Rev. Mod. Phys.* **78**, 865–951 (2006).
5. R. Bertoncini and A. P. Jauho, Gauge-invariant formulation of the intracollisional field effect including collisional broadening, *Phys. Rev. B* **44**, 3655-3664 (1991).
6. J. K. Freericks, V. M. Turkowski, and V. Zlatić, Real-time formalism for studying the nonlinear response of "smart" materials to an electric field, *Proceedings of the HPCMP Users Group Conference 2005, Nashville, TN, June 28–30, 2005*, edited by D. E. Post (IEEE Computer Society, Los Alamitos, CA, 2005), pp. 25–34.
7. V. M. Turkowski and J. K. Freericks, Spectral moment sum rules for strongly correlated electrons in time-dependent electric fields, *Phys. Rev. B* **73**, 075108 (2006); Erratum: *Phys. Rev. B* **73**, 209902(E) (2006).
8. J. K. Freericks, V. M. Turkowski, and V. Zlatić, Nonequilibrium dynamical mean-field theory, to appear in *Phys. Rev. Lett.* (*preprint cond-mat/0607053*).
9. J. K. Freericks, V. M. Turkowski, and V. Zlatić, Nonlinear response of strongly correlated materials to large electric fields, in *Proceedings of the HPCMP Users Group Conference 2006, Denver, CO, June 26–29, 2006*, edited by D. E. Post (IEEE Computer Society, Los Alamitos, CA, 2006), *to appear*.
10. U. Brandt and C. Mielsch, Thermodynamics of the Falicov-Kimball model in large dimensions II, *Z. Phys. B: Condens. Matter* **79**, 295–299 (1990).
11. U. Brandt and C. Mielsch, Free energy of the Falicov-Kimball model in large dimensions, *Z. Phys. B: Condens. Matter* **82**, 37–41 (1991).
12. M. Jarrell, Hubbard model in infinite dimensions: A quantum Monte Carlo study, *Phys. Rev. Lett.* **69**, 168–171 (1992).
13. M. J. Rozenberg, X. Y. Zhang, and G. Kotliar, Mott-Hubbard transition in infinite dimensions, *Phys. Rev. Lett.* **69**, 1236–1239 (1992).
14. R. Bulla, Zero temperature metal-insulator transition in the infinite-dimensional Hubbard model, *Phys. Rev. Lett.* **83**, 136–139 (1999).
15. M. Jarrell, Symmetric periodic Anderson model in infinite dimensions, *Phys. Rev. B* **51**, 7429-7440 (1995) .
16. Th. Pruschke, R. Bulla, and M. Jarrell, Low-energy scale of the periodic Anderson model, *Phys. Rev. B* **61**, 12799–12809 (2000).
17. J. K. Freericks, M. Jarrell, and D. J. Scalapino, Holstein model in infinite dimensions, *Phys. Rev. B* **48**, 6302–6314 (1993).
18. D. Meyer, A. C. Hewson, and R. Bulla, Gap Formation and Soft Phonon Mode in the Holstein Model, *Phys. Rev. Lett.* **89**, 196401 (2002).
19. J. K. Freericks and V. Zlatić, Exact dynamical mean field theory of the Falicov-Kimball model, *Rev. Mod. Phys.* **75**, 1333–1382 (2003).
20. P. Schmidt and H. Monien, Nonequilibrium dynamical mean-field theory of a strongly correlated system, *preprint cond-mat/0202046*.
21. L. M. Falicov and J. C. Kimball, Simple model for semiconductor-metal transitions: $SmB_6$ and Transition-Metal Oxides, *Phys. Rev. Lett.* **22**, 997–999

(1969).
22. T. Kennedy and E. H. Lieb, An itinerant electron model with crystalline or magnetic long range order, *Physica A* **138**, 320–358 (1986).
23. L. P. Kadanoff and G. Baym, *Quantum Statistical Mechanics* (Benjamin, New York, 1962).
24. L. V. Keldysh, Diagram technique for nonequilibrium processes, *Zh. Eksp. Teor. Fiz.* **47**, 1515–1527 (1964) [*Sov. Phys.-JETP* **20**, 1018–1026 (1965)].
25. J. Rammer and H. Smith, Quantum field-theoretical methods in transport theory of metals, *Rev. Mod. Phys.* **58**, 323–359 (1986).
26. M. Wagner, Expansions of nonequilibrium Greens functions, *Phys. Rev. B* **44**, 6104–6117 (1991).
27. W. Metzner, Linked-cluster expansion around the atomic limit of the Hubbard model, *Phys. Rev. B* **43**, 8549–8563 (1991).
28. D. C. Langreth, Linear and Non-Linear Response Theory with Applications, in *Linear and Nonlinear Electron Transport in Solids*, NATO Advanced Study Institute Series B, Vol. **17**, edited by J. T. Devreese and E. van Doren (Plenum, New York/London, 1976), p. 3–32.
29. D. O. Demchencko, A. V. Joura, and J. K. Freericks, Effect of particle-hole asymmetry on the Mott-Hubbard metal-insulator transition, *Phys. Rev. Lett.* **92**, 216401 (2004).
30. R. E. Peierls, On the theory of the diamagnetism of conduction electrons, *Z. Phys.* **80**, 763–791 (1933); A. P. Jauho and J. W. Wilkins, Theory of high-electric-field quantum transport for electron-resonant impurity systems, *Phys. Rev. B* **29**, 1919–1938 (1984).
31. V. Turkowski and J. K. Freericks, Nonlinear response of Bloch electrons in infinite dimensions, *Phys. Rev. B* **71**, 085104 (2005).
32. P. Schmidt, Time-dependent dynamical mean-field theory, *Diplome thesis*, University of Bonn (1999).
33. E. Wigner, On the Quantum Correction For Thermodynamic Equilibrium, *Phys. Rev.* **40**, 749–759 (1932).
34. H. Haug and A.-P. Jauho, *Quantum Kinetics in Transport and Optics of Semiconductors* (Springer-Verlag, Berlin/Heidelberg, 1996).
35. F. Bloch, On the quantum mechanics of electrons in crystal lattices, *Z. Phys.* **52**, 555–600 (1928).
36. C. Zener, A Theory of the Electrical Breakdown of Solid Dielectrics, *Proc. R. Soc. (London) Ser. A* **145**, 523–529 (1934).
37. N. W. Ashcroft and N. D. Mermin, *Solid State Physics* (Holt, Rinehart and Winston, New York, 1976).
38. G. H. Wannier, Dynamics of Band Electrons in Electric and Magnetic Fields, *Rev. Mod. Phys.* **34**, 645–655 (1962).
39. J. K. Freericks and V. M. Turkowski, Steady state nonequilibrium dynamical mean-field theory and the quantum Boltzmann equation, *J. Phys.: Confer. Ser.* **35**, 39–52 (2006).
40. V. Turkowski and J.K. Freericks, Nonequilibrium perturbation theory of the spinless Falicov-Kimball model, *preprint, cond-mat/0610640*.